Title	Thermodynamic Evaluation of Nano-Particle Binary Alloy Phase Diagrams
Author(s)	Tanaka, Toshihiro; Hara, Shigeta
Citation	Zeitschrift für Metallkunde. 2001, 92(11), p. 1236-1241
Version Type	VoR
URL	https://hdl.handle.net/11094/26514
rights	©Carl Hanser Verlag, München
Note	

Toshihiro Tanaka, Shigeta Hara
Department of Materials Science and Processing, Graduate School of Engineering, Osaka University, Osaka, Japan

Thermodynamic Evaluation of Nano-Particle Binary Alloy Phase Diagrams

Nano-particle binary alloy phase diagrams have been evaluated from the information on the Gibbs energy and the surface tension of the bulk size on the basis of the regular solution model. As the size of the particle decreases, the liquid-phase region is enlarged in those binary phase diagrams, in other words, the liquidus temperature decreases. Effect of the size of the particle on the phase equilibria is remarkable when the excess Gibbs energy is positive and its absolute value is large in solid and liquid phases.

Keywords: Surface tension; Regular solution model; Solid-liquid equilibria; Nano-particle; Thermodynamics

1 Introduction

It has been known that the melting point of pure metals decreases as the size of the metal particles becomes smaller [67Wro, 71Sam, 72Coo, 76Buf, 80All, 86All, 88Sak, 91Sas] since Takagi found this phenomenon for pure Pb and Bi [54Tak]. Thermodynamic evaluation has been also carried out to investigate the effect of the particle size on the melting point of pure metals [09Paw, 48Rei, 60Han, 77Cou].

In our previous work [01Tan2], we evaluated the binary phase diagrams of small-size particle systems when the phase diagrams consist of liquid phase and pure solid phases, for example, Cu–Pb, Cu–Bi and Au–Si alloys. From the information on the composition and temperature dependence of the surface tension of the liquid phase, the nano-particle binary phase diagrams can be calculated with the thermodynamic databases, which contain a lot of information on the Gibbs energy to evaluate the phase diagrams of the bulk size.

On the surface tension, the authors had already applied those thermodynamic databases to the evaluation of the surface tension of liquid alloys and molten ionic mixtures, and the interfacial tension between liquid steel and molten slag [94Tan, 96Tan, 98Tan1, 98Tan2, 98Tan3, 99Tan1, 99Tan2, 99Tan3, 99Ued, 01Tan1, 01Tan2]. From the above evaluations on the small-particle binary phase diagrams [01Tan2], we found

1. The liquid phase region of phase diagrams is enlarged as the size of the particle becomes smaller. The change in the phase diagrams with the particle size is remarkable when the size of the particle is below 100 nm.
2. In alloys, of which the composition dependence of the surface tension of the liquid phase shows large downward curvature, such as Cu–Pb and Cu–Bi alloys, the size of the particle influences largely the phase relations. On the other hand, in Au–Si alloys, of which the surface tension of the liquid phase changes smoothly with the composition, the effect of the size on the phase relations is not so large. The composition dependence of the surface tension is mainly determined from the excess Gibbs energy of the liquid phase.

In the previous work [01Tan2], we focused on some binary alloys, of which phase diagrams consist of liquid phase and pure solid phases, and the solid solutions have not been considered yet. We, however, need to make clear the effect of the excess Gibbs energy on the nano-particle binary phase diagrams including solid solutions more deeply. Pelton and Thompson [75Pel] have evaluated the binary phase diagrams in the bulk size systems by using the regular solution model when various values of the interaction parameter of the model in both liquid and solid phases were selected to elucidate the effect of the excess Gibbs energy on the binary phase diagrams, in which the melting points of the components are fixed.

The purpose of the present work is to examine the effect of the excess Gibbs energy in both liquid and solid phases on the nano-particle binary alloy phase diagrams on the basis of the regular solution model.

2 Thermodynamic Equations

Liquid-solid phase equilibria are evaluated in the present work. When a pure solid phase is selected as the reference state of Gibbs energy, the total Gibbs energies in liquid and solid phases, $\Delta G^{\mathrm{Total,Liq}}$ and $\Delta G^{\mathrm{Total,Sol}}$, of an alloy system in a small particle with its radius r are described in the following Eqs. (1)–(6) [01Tan2]:

$$\Delta G^{\mathrm{Total,Liq}} = \Delta G^{\mathrm{Bulk,Liq}} + \Delta G^{\mathrm{Surface,Liq}} \tag{1}$$

$$\Delta G^{\mathrm{Total,Sol}} = \Delta G^{\mathrm{Bulk,Sol}} + \Delta G^{\mathrm{Surface,Sol}} \tag{2}$$

The Gibbs energies of the bulk of an A–B binary alloy in liquid and solid phases, $\Delta G^{\mathrm{Bulk,Liq}}$ and $\Delta G^{\mathrm{Bulk,Sol}}$ in Eqs. (1) and (2), which correspond to $\Delta G^{\mathrm{Total,P}}$ (P = Liq or Sol) with $r = \infty$, are expressed in Eqs. (3) and (4).

$$\Delta G^{\mathrm{Bulk,Liq}} = N_{\mathrm{A}}\,\Delta G_{\mathrm{A}}^{\mathrm{LS}} + N_{\mathrm{B}}\,\Delta G_{\mathrm{B}}^{\mathrm{LS}} + G^{\mathrm{Excess,Liq}} + RT(N_{\mathrm{A}}\ln N_{\mathrm{A}} + N_{\mathrm{B}}\ln N_{\mathrm{B}}) \tag{3}$$

$$\Delta G^{\mathrm{Bulk,Sol}} = G^{\mathrm{Excess,Sol}} + RT(N_{\mathrm{A}}\ln N_{\mathrm{A}} + N_{\mathrm{B}}\ln N_{\mathrm{B}}) \tag{4}$$

where ΔG_A^{LS} and $\Delta G_B^{LS}$are Gibbs energies of pure components A and B in liquid phases relative to those of pure solid phases, in other words, the Gibbs energy of the melting. $G^{\mathrm{Excess,Liq}}$ and $G^{\mathrm{Excess,Sol}}$ are the excess Gibbs energies of liquid and solid phases in the A-B alloy, N_A and N_B are the mole fractions of components A and B, and R is the gas constant.

$\Delta G^{\mathrm{Surface,Liq}}$ and $\Delta G^{\mathrm{Surface,Sol}}$ in Eqs. (1) and (2), the effect of the surface on $\Delta G^{\mathrm{Total,P}}$, are assumed as follows [01Tan2]:

$$\Delta G^{\mathrm{Surface.Liq}} = \frac{2\sigma^{\mathrm{Liq}} V^{\mathrm{Liq}}}{r} - \frac{2(N_A \sigma_A^{\mathrm{Sol}} V_A^{\mathrm{Sol}} + N_B \sigma_B^{\mathrm{Sol}} V_B^{\mathrm{Sol}})}{r} \tag{5}$$

$$\Delta G^{\mathrm{Surface.Sol}} = \frac{2\sigma^{\mathrm{Sol}} V^{\mathrm{Sol}}}{r} - \frac{2(N_A \sigma_A^{\mathrm{Sol}} V_A^{\mathrm{Sol}} + N_B \sigma_B^{\mathrm{Sol}} V_B^{\mathrm{Sol}})}{r} \tag{6}$$

where r is the radius of a particle, σ^{Liq} and σ^{Sol} are the surface tensions of liquid and solid alloys, V^{Liq} and V^{Sol} are the molar volumes of liquid and solid alloys, σ_A^{Sol} and σ_B^{Sol} are the surface tensions of pure solid A and B, and V_A^{Sol} and V_B^{Sol} are the molar volumes of pure solid A and B.

Although the excess Gibbs energies stored in thermodynamic databases, which are used for the calculation of phase diagrams of the bulk, were used in the previous work [01Tan2], the regular solution model is applied in the present work because various interaction energies can be selected easily as follows:

$$G^{\mathrm{Excess,Liq}} = N_A N_B \Omega_{AB}^{\mathrm{Liq}} \tag{7}$$

$$G^{\mathrm{Excess,Sol}} = N_A N_B \Omega_{AB}^{\mathrm{Sol}} \tag{8}$$

where $\Omega_{AB}^{\mathrm{Liq}}$ and $\Omega_{AB}^{\mathrm{Sol}}$ are the interaction energies in liquid and solid phases.

Since Pelton and Thompson [75Pel] assumed the simple equation of the Gibbs energy of the melting in their evaluation of phase diagrams, we also use the following equations as they applied:

$$\Delta G_A^{LS} = T_{A,mp} \cdot S_{A,mp} - T \cdot S_{A,mp} \tag{9}$$

$$\Delta G_B^{LS} = T_{B,mp} \cdot S_{B,mp} - T \cdot S_{B,mp} \tag{10}$$

where $T_{X,mp}$ and $S_{X,mp}$ are the melting point and the entropy of fusion for pure substance X (X = A or B).

In the present work, $S_{X,mp}$ is roughly assumed to be $10\ \mathrm{J \cdot K^{-1} mol^{-1}}$ according to Richard's rule [95Gas]. In addition, we select here $T_{A,mp} = 1200$ K and $T_{B,mp} = 600$ K.

For the surface tension of pure liquid metals at their melting points, the following approximation has been reported [88Iid] :

$$\sigma_{X,mp}^{\mathrm{Liq}}(\mathrm{Nm^{-1}}) = 4.8 \times 10^{-8} R \frac{T_{X,mp}/\mathrm{K}}{\{V_{X,mp}/\mathrm{m^3\ mol^{-1}}\}^{2/3}} \tag{11}$$

where $\sigma_{X,mp}^{\mathrm{Liq}}$ and $V_{X,mp}$ are the surface tension and the molar volume of the element X at its melting point. When we select $V_{X,mp} = 10 \times 10^{-6}\ \mathrm{m^3 mol^{-1}}$, as described below, the following rough relation is obtained from Eq. (11):

$$\sigma_{X,mp}^{\mathrm{Liq}}(\mathrm{Nm^{-1}}) = T_{X,mp}/1000 \tag{12}$$

In addition, the temperature coefficient of the surface tension of pure liquid has been reported to be about $0.0001\ \mathrm{Nm^{-1}K^{-1}}$ [88Iid]. Thus, we assumed the following equation for σ_A^{Liq} and σ_B^{Liq} in the present work:

$$\sigma_A^{\mathrm{Liq}} = 1.2 - 0.0001 \cdot (T - T_{A,mp})/\mathrm{Nm^{-1}} \quad (T_{A,mp} = 1200\,\mathrm{K}) \tag{13}$$

$$\sigma_B^{\mathrm{Liq}} = 0.6 - 0.0001 \cdot (T - T_{B,mp})/\mathrm{Nm^{-1}} \quad (T_{B,mp} = 600\,\mathrm{K}) \tag{14}$$

For the surface tension σ_X^{Sol} of pure solid X, the following equation was used in the previous work [01Tan2]:

$$\sigma_X^{\mathrm{Sol}} = 1.25 \cdot \sigma_{X,mp}^{\mathrm{Liq}} + \frac{\partial \sigma_X^{\mathrm{Liq}}}{\partial T}(T - T_{X,mp}) \quad (X = A \text{ or } B) \tag{15}$$

In Eq. (15), we assumed the following:

1. The value of σ_X^{Sol} of pure solid metals at the melting point is found to be 25 % larger than that of pure liquid metals on the average.
2. The temperature dependence of σ_X^{Sol} is assumed to be the same as that of σ_X^{Liq}.
3. The effects of crystal faces on σ_X^{Sol} are ignored.

From Eqs. (13)–(15), the following relations are obtained:

$$\sigma_A^{\mathrm{Sol}} = 1.25 \times 1.2 - 0.0001 \cdot (T - T_{A,mp})/\mathrm{Nm^{-1}} \tag{16}$$

$$\sigma_B^{\mathrm{Sol}} = 1.25 \times 0.6 - 0.0001 \cdot (T - T_{B,mp})/\mathrm{Nm^{-1}} \tag{17}$$

For the molar volume, we used the following values by assuming that the temperature dependence of the molar volume and the volume change due to the melting are neglected because the effect of the excess Gibbs energy and the surface tension on the phase equilibria is focused in the present work.

$$V_A^{\mathrm{Liq}} = V_B^{\mathrm{Liq}} = 10 \times 10^{-6}/\mathrm{m^3 mol^{-1}} \tag{18}$$

$$V_A^{\mathrm{Sol}} = V_B^{\mathrm{Sol}} = 10 \times 10^{-6}/\mathrm{m^3 mol^{-1}} \tag{19}$$

It is assumed that the molar volumes of liquid alloy V^{Liq} and solid alloy V^{Sol} in Eqs. (5) and (6) are obtained from the following simple additivities:

$$V^{\mathrm{Liq}} = N_A V_A^{\mathrm{Liq}} + N_B V_B^{\mathrm{Liq}} \tag{20}$$

$$V^{\mathrm{Sol}} = N_A V_A^{\mathrm{Sol}} + N_B V_B^{\mathrm{Sol}} \tag{21}$$

The surface tensions of liquid and solid alloy, σ^P (P = Liq or Sol), are evaluated from Butler's equation [32But] as follows [96Tan, 98Tan1, 98Tan2, 98Tan3, 99Tan1, 99Tan2]:

$$\sigma^P = \sigma_A^P + \frac{RT}{A_A} \ln \frac{N_A^{\mathrm{Surf}}}{N_A} + \frac{1}{A_A} G_A^{\mathrm{E,P,Surf}}(T, N_B^{\mathrm{Surf}}) - \frac{1}{A_A} G_A^{\mathrm{E,P,Bulk}}(T, N_B) \tag{22a}$$

$$\sigma^P = \sigma_B^P + \frac{RT}{A_B} \ln \frac{N_B^{\mathrm{Surf}}}{N_B} + \frac{1}{A_B} G_B^{\mathrm{E,P,Surf}}(T, N_B^{\mathrm{Surf}}) - \frac{1}{A_B} G_B^{\mathrm{E,P,Bulk}}(T, N_B) \tag{22b}$$

Butler derived the above equation, assuming that the outermost monolayer of a material is the hypothetical "surface". In Eqs. (22a) and (22b), N_B^{Surf} is the mole fraction of element B in the surface considered by Butler [32But]. $A_X = LN_0^{1/3}(V_X^P)^{2/3}$ (N_0 = Avogadro number; X = A or B; $L = 1.091$) is the molar surface area of pure X, and this is obtained from the molar volume V_X^P. $G_X^{E,P,Bulk}(T, N_B)$ and $G_X^{E,P,Surf}(T, N_B^{Surf})$ are the partial excess Gibbs energies of component X in the bulk and the surface, respectively, as functions of T and N_B or N_B^{Surf} (P = Liq or Sol). $G_X^{E,P,Bulk}(T, N_B)$ can be obtained from the following relations:

$$G_A^{E,P,Bulk}(T, N_B) = G^{Excess,P} - N_B \frac{\partial G^{Excess,P}}{\partial N_B} \tag{23a}$$

$$G_B^{E,P,Bulk}(T, N_B) = G^{Excess,P} + (1 - N_B) \frac{\partial G^{Excess,P}}{\partial N_B} \tag{23b}$$

For the excess Gibbs energy in the surface $G_X^{E,P,Surf}(T, N_B^{Surf})$, we derived the following equations [96Tan, 98Tan1, 98Tan2, 98Tan3, 99Tan1, 99Tan2, 99Tan3, 99Ued, 01Tan1, 01Tan2] based on the model proposed by Yeum et al. [89Yeu].

$$G_X^{E,P,Surf}(T, N_B^{Surf}) = \beta^{MIX} \cdot G_X^{E,P,Bulk}(T, N_B^{Surf}) \tag{24}$$

$$\beta^{MIX} = 0.83 : \text{for liquid alloys} \tag{25}$$

Equation (24) means that $G_X^{E,P,Surf}(T, N_B^{Surf})$, which has the same formula as $G_X^{E,P,Bulk}(T, N_B)$, is obtained by replacing N_B by N_B^{Surf} in $G_X^{E,P,Bulk}(T, N_B)$ (X = A or B), and then multiplying β^{MIX} to $G_X^{E,P,Bulk}(T, N_B^{Surf})$. β^{MIX} is a parameter corresponding to the ratio of the coordination number in the surface to that in the bulk considering the surface relaxation [96Tan, 98Tan1, 98Tan2, 98Tan3, 99Tan1, 99Tan2, 99Tan3, 99Ued]. For the solid solutions, we assume the following value as $\beta^{MIX}$by assuming the close-packed structure in the present work because the coordination number in the bulk is 12 and that in the surface is 9:

$$\beta^{MIX} = 9/12 = 0.75 : \text{for solid alloys} \tag{26}$$

The surface tension σ^P of liquid or solid alloy can be calculated from Eqs. (22), (24)–(26) as follows:

1. Setting temperature $T$and composition N_B of a solution.
2. Inserting the values for surface tension σ_X^P and molar volume V_X^P (P = Liq or Sol) of pure substances at the above temperature in Eqs. (22a) and (22b).
3. Determining the excess Gibbs energies in the bulk phase at the above temperature and composition, and substituting them in Eqs. (22a) and (22b).
4. Then, Eqs. (22a) and (22b) become the simultaneous equations with unknown N_B^{Surf} and σ^P. These equations are solved for those unknown N_B^{Surf} and σ^P numerically.

3 Calculation of Phase Diagrams in Nano-Particle Systems

Liquid-solid phase equilibria are obtained from the following thermodynamic conditions :

$$\mu_A^{Total,Liq} = \mu_A^{Total,Sol} \tag{27}$$

$$\mu_B^{Total,Liq} = \mu_B^{Total,Sol} \tag{28}$$

$$\mu_A^{Total,P} = \Delta G^{Total,P} - N_B \frac{\partial \Delta G^{Total,P}}{\partial N_B} \quad (\text{P} = \text{Liq or Sol}) \tag{29}$$

$$\mu_B^{Total,P} = \Delta G^{Total,P} + (1 - N_B) \frac{\partial \Delta G^{Total,P}}{\partial N_B} \quad (\text{P} = \text{Liq or Sol}) \tag{30}$$

Table 1 summarizes the parameters used for the present calculation of the phase diagrams. As shown in this table, the melting points of pure components A and B are fixed to be 1200 and 600 K, respectively. The entropy of melting is also fixed to be 10 J K^{-1}mol^{-1}. The surface tension and the molar volume of pure components are selected in Eqs. (13)–(19) as mentioned above. The interaction parameters Ω_{AB}^{Liq} and Ω_{AB}^{Sol} are changed from −20 to 30 kJ as shown in Figs. 2 and 3 which are described below in detail.

Table 1. Parameters used in the calculation of phase diagrams.

Substance	Melting point K	Entropy of fusion JK^{-1}mol^{-1}	Surface Tension Nm^{-1}	Molar volume m^{3}mol^{-1}
A	1200	10	1.2−0.0001(T−1200): for Liq 1.2×1.25−0.0001(T−1200): for Sol	10×10^{-6}: for Liq 10×10^{-6}: for Sol
B	600	10	0.6−0.0001(T−600): for Liq 0.6×1.25−0.0001(T−600): for Sol	10×10^{-6}: for Liq 10×10^{-6}: for Sol

Ω_{AB}^{Liq} kJ	Ω_{AB}^{Sol}/kJ			
	30	15	0	−15
20	Fig. 3a			
10	Fig. 3b			
0	Figs. 2c, 3c	Fig. 2b	Fig. 2a	
−20	Fig. 3d			Fig. 2d

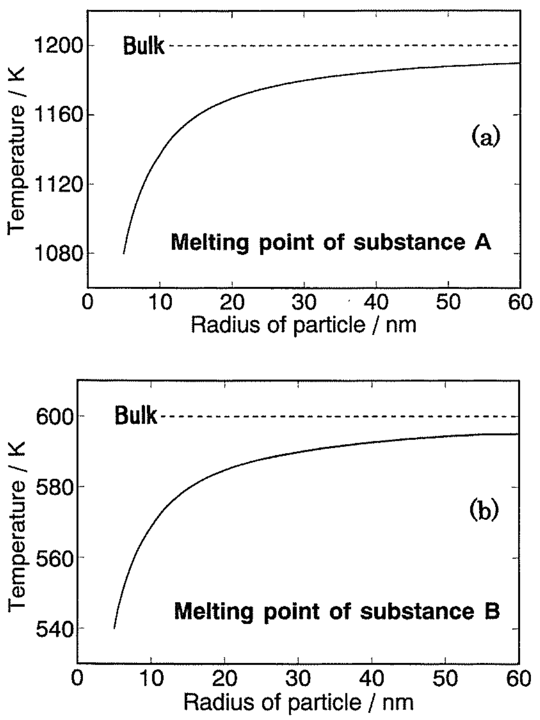

Fig. 1. Change in the melting point of pure substances A (a) and B (b) with the particle radius.

The change in the melting point of the pure substance with radius r of the particle can be evaluated from the following Eq. (31), which is obtained from Eqs. (1), (3) and (5) for the pure substance X:

$$\Delta G^{\text{Total,Liq}} = \Delta G^{\text{Bulk,Liq}} + \Delta G^{\text{Surface,Liq}}$$

$$= \Delta G_{X}^{LS} + \frac{2\sigma_{X}^{\text{Liq}}V_{X}^{\text{Liq}}}{r} - \frac{2\sigma_{X}^{\text{Sol}}V_{X}^{\text{Sol}}}{r} \qquad (31)$$

The temperature T which gives $\Delta G^{\text{Total,Liq}} = 0$ in Eq. (31) is the melting point of pure X at a given radius r of a particle. The size dependence of the melting points of the substances A and B, of which physical properties are given in Eqs. (9)–(19), is shown in Figs. 1a and b. The change in the melting point with the particle size for pure Au calculated from the above Eq. (31) agrees well with the experimental result [71Sam], as described in our previous work [01Tan2]. Usually, pure metals have the following order of ΔG_{X}^{LS}, σ_{X}^{P} and V_{X}^{P} (P = Liq or Sol):

ΔG_{X}^{LS}: about $10^{3}-10^{4}$ J mol

σ_{X}^{P}: about 1 Nm^{-1}

V_{X}^{P}: about $1\times10^{-6}-10\times10^{-6}\ \text{m}^{3}\text{mol}^{-1}$

Thus, when the radius of the particle r is around $1\times10^{-9}-10\times10^{-9}$m , in other words, r is of nano-size order, $\Delta G^{\text{Surface,P}}$ has the same order of $\Delta G^{\text{Bulk,P}}$, which means that the effect of the size of the particle on the phase equilibria is noticeable when r decreases below 100 nm.

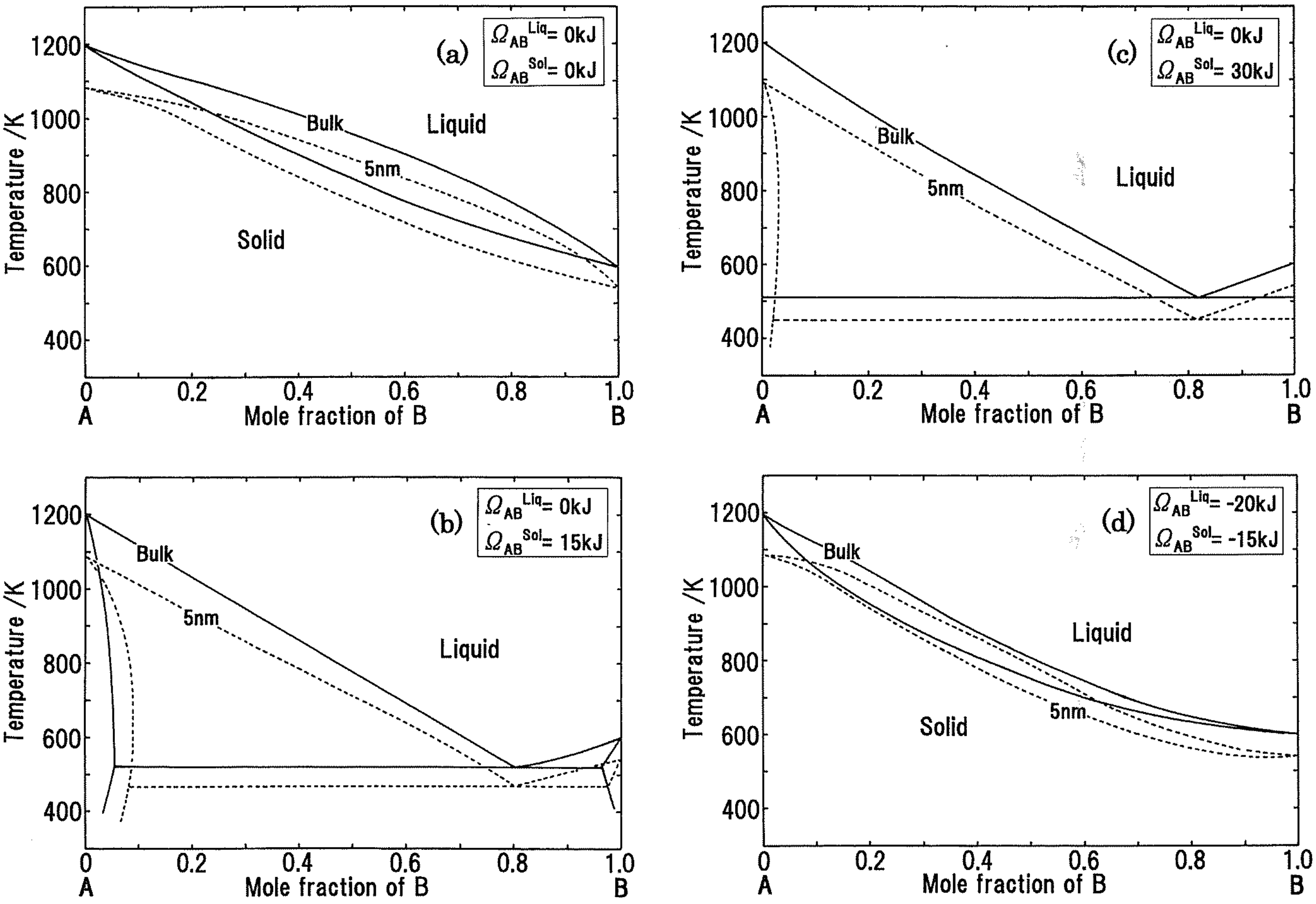

Fig. 2. Calculated results of the phase diagrams with systematic change of Ω_{AB}^{Liq} and Ω_{AB}^{Sol} on the basis of the regular solution model (a–d).

Figures 2 and 3 show the calculated results of the phase diagrams by using the parameters in Table 1. In these figures, the solid curves indicate the phase equilibria in the bulk ($r = \infty$). On the other hand, the chain and the dotted curves are the calculated results for r = 10 nm and 5 nm, respectively. Figure 2a indicates the phase diagrams for the ideal solutions in both solid and liquid phases, in other words, $\Omega_{AB}^{Liq} = \Omega_{AB}^{Sol} = 0$. When Ω_{AB}^{Sol} increases from 0 to 30 kJ with $\Omega_{AB}^{Liq} = 0$, the phase diagrams change as shown in Figs. 2b and c. Figure 2d shows the phase diagrams for $\Omega_{AB}^{Liq} = -20$ kJ and $\Omega_{AB}^{Sol} = -15$ kJ as an example for $\Omega_{AB}^{Liq} < 0$ and $\Omega_{AB}^{Sol} < 0$.

When Ω_{AB}^{Sol} is fixed to be 30 kJ and Ω_{AB}^{Liq} changes from +20 to −20 kJ, the phase diagrams are obtained as shown in Figs. 3a–d. As can be seen in Fig. 3, when the interaction parameters are $\Omega_{AB}^{Liq} \gg 0$ and $\Omega_{AB}^{Sol} \gg 0$, the effect of the particle size on the phase diagrams is remarkable. As described in the previous works [94Tan, 96Tan, 98Tan1, 98Tan2, 98Tan3, 99Tan1, 99Tan2, 99Tan3, 99Ued, 01Tan1, 01Tan2], the liquid or solid alloys indicate the large downward curvature of the composition dependence of the surface tension in the conditions of $\Omega_{AB}^{Liq} \gg 0$ and $\Omega_{AB}^{Sol} \gg 0$. This composition dependence of the surface tension affects the contribution of $\Delta G^{Surface,P}$ to $\Delta G^{Total,P}$. Especially, when $\Omega_{AB}^{Sol} \gg 0$, in other words, the excess Gibbs energy of the solid solution is positive and its absolute value is large, the solid solutions do not appear in some of the phase diagrams of the bulk as shown in Figs. 2c, 3c and 3d. However, when the particle size decreases, the contribution of $\Delta G^{Surface,Sol}$ to $\Delta G^{Total,Sol}$ in the solid phase cannot be ignored. Consequently, as shown in Figs. 2 and 3, the solid solution appears in the small-particle systems even when the bulk phase diagrams do not show the solid solutions.

In addition, the solid solution region is enlarged as the size of the particle becomes smaller. Therefore, the small-particle binary phase diagrams in Cu–Pb, Cu–Bi and Au–Si alloys obtained in our previous work [01Tan2] might be corrected by considering the solid solutions although the solid solutions are not considered in the previous evaluations of those phase diagrams. However, we need the exact information on the excess Gibbs energy of the solid solutions of those alloys, which can be ignored for the bulk phase diagrams.

In addition, we have to pay careful attention to the procedure to evaluate the surface tension $\sigma^S$of the solid solution although Eq. (26) is used to evaluate σ^S in the present work. We have already confirmed the validity of the procedure to calculate the surface tension σ^L of liquid alloys by comparing the calculated results of σ^L with experimental values [94Tan, 96Tan, 99Tan1, 01Tan1], but Eq. (26) for σ^S is only a trial as an approximation. As described above, the phase diagrams of binary alloys in the nano-particle systems can be evaluated from the information on the Gibbs energy and the surface tension of the bulk phase although the following rough assumptions have been still used in the present work:

1. Quantum effect on the nano-particle is not considered.
2. The effect of the curvature of the particle on the surface tension is neglected although it has been reported that

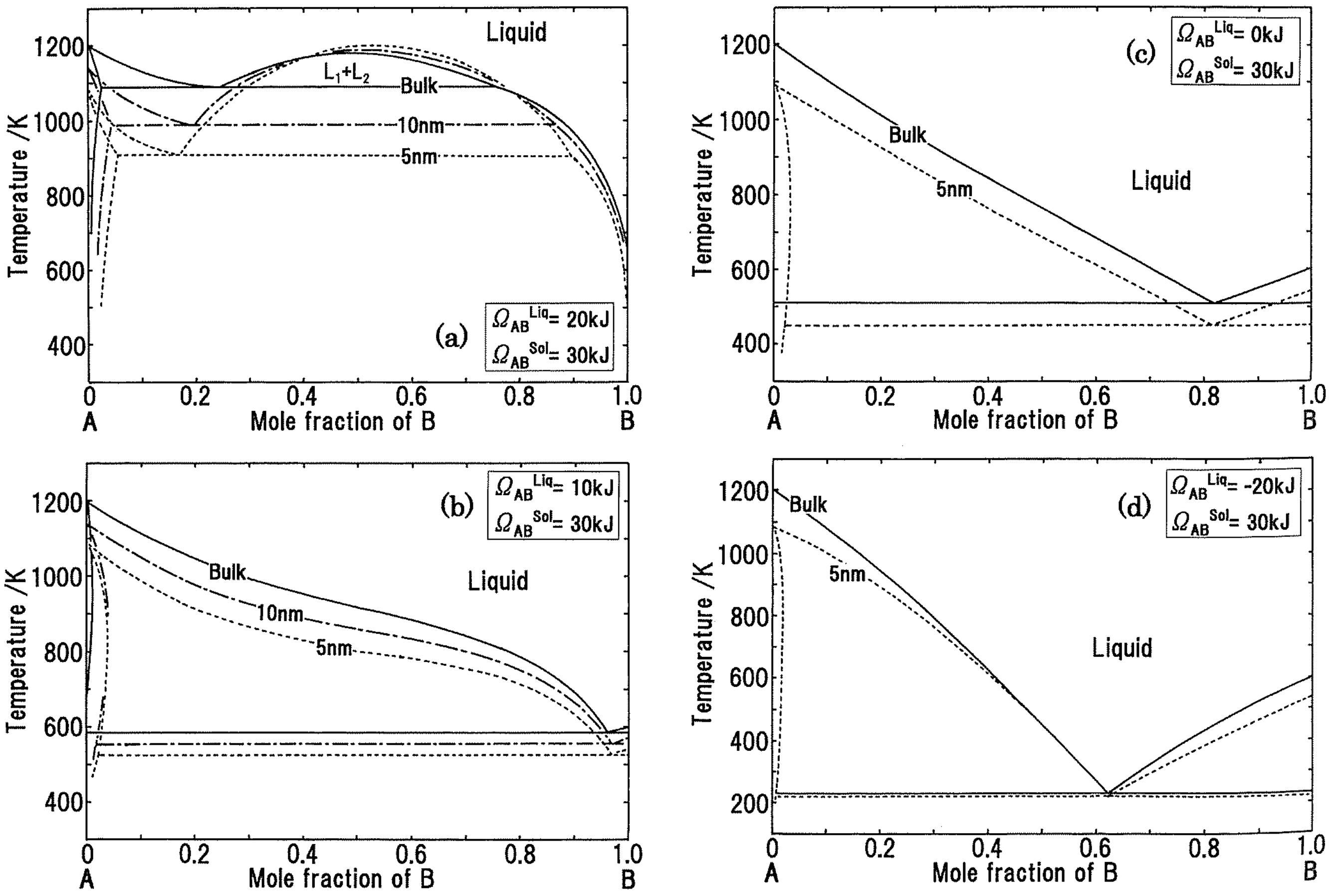

Fig. 3. Calculated results of the phase diagrams with systematic change of Ω_{AB}^{Liq}, and $\Omega_{AB}^{Sol} = 30$ kJ on the basis of the regular solution model (a–d).

the value of the surface tension is influenced by the curvature of the surface in a small particle especially below $r = 5$ nm [49Tol, 79Mor, 89Gla].

3. The effects of crystal faces on the surface properties of solid phases are ignored.
4. The relation between the surface tension of solid at the melting point and that of liquid as well as the temperature dependence of the surface tension of solid is assumed to be common for all kinds of substances.

4 Concluding Remarks

The nano-particle binary alloy phase diagrams were evaluated from the information on the Gibbs energy and the surface tension of the bulk phase on the basis of the regular solution model although some rough approximations have been applied in the present work. The surface tensions of liquid and solid alloys are also calculated from the Gibbs energy of the bulk in the above evaluation. The effect of the size of the particle on the phase equilibria is conspicuous when the excess Gibbs energies in solid and liquid phases are positive and their absolute values are large. Even when the solid solutions are not apparently found in the phase diagrams of the bulk systems, the contribution of the Gibbs energy of the solid solution to the phase equilibria cannot be ignored in the small-particle systems.

References

09Paw Pawlow, P.: Z. Phys. Chem. 65 (1909) 1–35.
32But Butler, J.A.V.: Proc. Roy. Soc. A 135 (1932) 348–375.
48Rei Reiss, H.; Wilson, I.B.: J. Colloid Sci. 3 (1948) 551–561.
49Tol Tolman, R.C.: J. Chim. Phys. 17 (1949) 333–337.
54Tak Takagi, M.: J. Phys. Soc. Jpn. 9 (1954) 359–363.
59All Allen, B.C.; Kingery, W.D.: Trans. Metall. Soc. AIME 215 (1959) 30–37.
60Han Hanszen, K.J.: Z. Phys. 157 (1960) 523–553.
62Swa Swalin, R.A.: Thermodynamics of Solids, John Wiley, New York (1962).
67Wro Wronski, C.R.M.: Brit. J. Appl. Phys. 18 (1967) 1731–1737.
71Sam Sambles, J.R.: Proc. Roy. Soc. Lond. A 324 (1971) 339–351.
72Coo Coombes, C.J.: J. Phys. F 2 (1972) 441–449.
72Wit Wittenberg, L.J.; DeWitt, R.: J. Chem. Phys. 56 (1972) 4526–4533.
75Pel Pelton, A.D.; Thompson, W.T.: Prog. Solid State Chem. 10 (1975) 119.
76Buf Buffat, Ph.; Borel, J-P.: Phys. Rev. 13 (1976) 2287–2298.
77Cou Couchman, P.R.; Jesser, W.A.: Nature 269 (1977) 481–483.
79Mor Morokhov, I.D.: Izv. Akad. Nauk SSSR Metall. No. 6 (1979) 159–161.
80All Allen, G.L.; Gile, W.W.; Jesser, W.A.: Acta Metall. 28 (1980) 1695–1701.
83Kum Kumikov, V.K.; Khokonov, Kh.B.: J. Appl. Phys. 54 (1983) 1346–1350.
86All Allen, G.L.; Bayles, R.A.; Gile, W.W.; Jesser, W.A.: Thin Solid Films 144 (1986) 297–308.
88Iid Iida, T.; Guthrie, R.I.L.: The Physical Properties of Liquid Metals, Clarendon Press, Oxford (1988) 71 and 132.
88Sak Saka, H.; Nishikawa, Y.; Imura, T.: Phil. Mag. A 57 (1988) 895–906.
89Yeu Yeum, K.S.; Speiser, R.; Poirier, D.R.: Metall. Trans. B 20 (1989) 693–703.
89Gla Gladkikh, N.T.; Grigoreva, L.K.; Dukarov, S.V.: Sov. Phys. Solid State 31 (1989) 728–733.
91Sas Sasaki, K.; Saka, H.: Phil. Mag. A 63 (1991) 1207–1220.
94Tan Tanaka, T.; Iida, T.: Steel Res. 65 (1994) 21–28.
95Gas Gaskell, D.R.: Introduction to the Thermodynamics of Materials, Taylor & Francis, Washington, DC (1995).
96Tan Tanaka, T.; Hack, K.; Iida, T.; Hara, S.: Z. Metallkd. 87 (1996) 380–389.
98Tan1 Tanaka, T.; Hara, S.; Ogawa, M.; Ueda, T.: Z. Metallkd. 89 (1998) 368–374.
98Tan2 Tanaka, T.; Hara, S.; Ogawa, M.; Ueda, T.: Molten Salt Forum 5–6 (1998) 213–216.
98Tan3 Tanaka, T.; Hara, S.; Ueda, T. in: P.C. Trulove, H.C. De Long, G.R. Stafford, S. Deki (eds.), Proc. 11th Int. Symp. on Molten Salts, San Diego, CA (1998) 645–650.
99Tan1 Tanaka, T.; Hack, K.; Hara,S.: MRS Bulletin 24 (1999) 45–50.
99Tan2 Tanaka, T.; Hara, S.: Electrochemistry 67 (1999) 573–580.
99Tan3 Tanaka, T.; Hara, S.: Z. Metallkd. 90 (1999) 348–354.
99Ued Ueda, T.; Tanaka, T.; Hara, S.: Z. Metallkd. 90 (1999) 342–347.
01Tan1 Tanaka, T.; Hack, K.; Hara,S.: Calphad 24 (2001) 465–474.
01Tan2 Tanaka, T.; Hara, S.: Z. Metallkd. 92 (2001) 467–472.

(Received June 15, 2001)

Correspondence Address

Prof. Dr. T. Tanaka
Department of Materials Science and Processing
2-1 Yamadaoka, Suita, Osaka 565–0871, Japan
Fax: +81 6 6879 7466
E-mail: tanaka@mat.eng.osaka-u.ac.jp